Aerocapture Mission Analysis

Engelsma, Jorrik; Mooij, Erwin

DOI
10.2514/6.2020-1740

Publication date
2020

Document Version
Final published version

Published in
AIAA Scitech 2020 Forum

AIAA SciTech Forum
6-10 January 2020, Orlando, FL
AIAA Scitech 2020 Forum

10.2514/6.2020-1740

Aerocapture Mission Analysis

Jorrik Engelsma* and Erwin Mooij†
Delft University of Technology, Faculty of Aerospace Engineering,
Kluyverweg 1, 2629 HS Delft, The Netherlands

By simulating full lift-up and full lift-down trajectories, the limit initial conditions for which successful aerocapture is possible have been determined. These boundaries form the entry corridor for aerocapture, and have been developed for Earth, Mars, and Venus. Moreover, two different vehicles representative for either manned missions or sample return were studied. The vehicle configurations were varied to study the effect of mass and lift on the size of the entry corridor. From this investigation it was determined that increasing the lift produced by the vehicle is a more effective method of widening the entry corridor than decreasing the mass. Furthermore, it was found that a lift-up-lift-down bang-bang type of trajectory minimises both the total ΔV, the load factor, and the heat load. An optimisation scheme was set up to determine the optimal switch time, which showed that for nearly all initial conditions that fall within the boundaries specified by the developed entry corridors, optimal aerocapture could indeed be achieved with an apoapsis correcting manoeuvre with a ΔV smaller than 0.01 m/s.

Nomenclature

C_D	Aerodynamic drag coefficient	[-]
C_L	Aerodynamic lift coefficient	[-]
CM	Command Module	
CRM	Crew Return Module	
SRM	Sample Return Module	
t_s	Switch time	[s]
t_f	time at atmospheric exit	[s]
t_p	time at point of deepest penetration	[s]
Δt_0	Initial time step	[s]
Δt_{min}	Minimal time step	[s]
Δt_{max}	Maximal time step	[s]
ΔV_1	Periapsis raising manoeuvre	[m/s]
ΔV_2	Apoapsis correcting manoeuvre	[m/s]

I. Introduction

In an attempt to reduce the cost of interplanetary missions without reducing payload mass, or to enable the exploration of far-away gas giants, the aerocapture manoeuvre has often been proposed and studied since its original introduction.[1] The objective of an aerocapture manoeuvre is to dissipate the orbital energy of the spacecraft by traversing through the atmosphere of a planet at high speed, and thus being captured with no or at most limited use of a propulsive system. Aerocapture can either target a landing site on the central body that the spacecraft reaches after a single pass through the atmosphere, or through skipping entry, or it can be used to orbit the target body.

In case of orbit targeting, after the spacecraft leaves the atmosphere it travels to the apoapsis of the post-atmospheric exit trajectory. After reaching the apoapsis, the spacecraft executes a propulsive manoeuvre to raise its periapsis out of the atmosphere. This manoeuvre requires a ΔV_1, and is also

*MSc Graduate Student, Section Astrodynamics and Space Missions.
†Assistant Professor, Section Astrodynamics and Space Missions, e.mooij@tudelft.nl, Associate Fellow AIAA.

Table 1. Apollo Command Module Aerodynamic Model.[2]

Mach no. [-]	Trim Angle of Attack [deg]	C_L [-]	C_D [-]
0.4	-12.86	0.24465	0.85300
0.7	-15.62	0.26325	0.98542
0.9	-18.30	0.32074	1.10652
1.1	-25.13	0.49373	1.16970
1.2	-24.87	0.47853	1.15600
1.35	-25.99	0.56282	1.27880
1.65	-26.78	0.55002	1.26570
2.0	-26.86	0.53247	1.27210
2.4	-26.38	0.0740	1.24120
3.0	-25.86	0.47883	1.21670
4.0	-23.88	0.44147	1.21480
10.0	-23.21	0.42856	1.2246
$\geq$ 29.5	-19.94	0.38773	1.28910

Table 2. Nominal values for the physical properties of the CRM and SRM. The CRM is based directly on the Apollo CM.[4]

Mission	Diameter [m]	Aerodynamic Reference Area [m^2]	Nose Radius [m]	Mass [kg]
CRM	3.9116	12.017	4.694	5500
SRM	0.75	0.441	0.90	38.77

labelled as such. The spacecraft then orbits to its periapsis, where it corrects the apoapsis using a velocity correction ΔV_2, if needed. When the aerocapture is optimal, it means that $\Delta V_2 = 0$.

In this paper the range of applicability for aerocapture missions for Earth, Mars, and Venus is investigated, for a vehicle representing a manned vehicle, and a vehicle used for sample return. The effects of varying the vehicle characteristics of this range of applications are studied, and a method for determining whether optimal aerocapture is possible for arbitrary vehicles and initial conditions is provided.

The layout of this paper is as follows. Section II will discuss the simulation model, consisting of the vehicle, flight environment, and simulation aspects. Section III introduces the fundamental aspects of the entry corridor, followed by the two types that are studied in this paper, *i.e.,* the altitude-targeting entry corridor, and the direct-entry entry corridor. These corridors are presented for Venus, Earth and Mars, and the effect of variations in aerodynamics and mass are considered. Finally, in Sec. IV optimal aerocapture trajectories are determined and analysed. Section V concludes this paper with some final remarks.

II. Simulation Model

A. Vehicle Definition

Two vehicles are considered, one representative of a vehicle capable of manned flight, hereinafter referred to as the Crew Return Module (CRM), and a smaller vehicle representative of a sample return capsule, hereinafter referred to as the Sample Return Module (SRM). The shape, aerodynamic properties, and mass of both vehicles are based on the Apollo Command Module (CM). For convenience, the aerodynamic characteristics of the Apollo CM are tabulated in Table 1.

The shape, size, and mass of the CRM are taken directly from the Apollo CM. The size of the SRM is modelled as a scaled-down version to more closely match the size of other sample return missions, specifically the vehicle proposed for the Mars Sample Return Mission.[3] The mass of the scaled-down version is estimated by approximating the volume of the Apollo CM capsule by a cone, and assuming a linear relation between the vehicle volume and mass. The used properties for both vehicles are listed in Table 2.

Both vehicles are subject to load-factor and heat-flux constraints. For the trajectories of the CRM a maximum load factor of 12g is imposed, and for the SRM a maximum load factor of 20g. For either vehicle a maximum heat flux of 7.95 MW/m^2 is considered.

B. Central Body Environments

Aerocapture manoeuvres about Earth, Mars, and Venus will be considered. These three bodies are chosen specifically as they provide different atmospheric densities ranging from very low on Mars, to very high on Venus. For each of the three central bodies, the shape of the body, the atmosphere surrounding the body, and the gravitational field induced by the massive body has to be modelled.

All three planets are defined to be rotating spheroids with a co-rotating atmosphere. For Earth and Mars the flattening of the poles is taken into account. For the Earth atmosphere the NRLMSISE-00 atmosphere model is used,[5] for Mars a latitude, longitude, and time-averaged version of the ESA Mars Climate Database[6] (EMCD), and for Venus a latitude, longitude, and time-averaged version of the Venus Global Reference Atmosphere Model[7] (VenusGRAM). The gravitational fields of Earth and Mars are modelled using a spherical harmonics model where only the J_2 term is taken into account, whereas the gravity of Venus is defined by a central field only.

Aeroheating relations to obtain an estimate for the convective and radiative heat flux are defined for all three atmospheres. The heat flux is intended to act as a thermal constraint for the trajectory in addition to the acceleration constraint, and therefore conservative models are selected. For the convective heat flux, the general relation for heat flux is modified using a hot-wall correction and applied using a conservative set of coefficients.[8–11] For the radiative heat flux, a particular relation is used for Earth and Mars,[12] and a different one for Venus.[13]

C. Trajectory Simulation

The trajectory simulation is performing using the Technical University of Delft Astrodynamical Toolbox, or TUDAT[a], a collection of astrodynamical simulation code developed and maintained by affiliates of Delft University of Technology. For each trajectory only the translational motion is simulated. The angle of attack is set at its trim value, as a function of Mach number, provided in Table 1, the bank angle is commanded by the guidance algorithm, and the angle of side-slip is set to zero throughout the entire flight. The full equations of motion representing the translational motion of the vehicle are integrated using a variable step-size 6^{th}-order Adams-Bashforth Adams-Moulton, linear multistep numerical integrator, with a tolerance of 10^{-10}.

Throughout this research ideal guidance, navigation, and control is assumed, resulting in instantaneous bank-angle switches. The vehicle always starts at an altitude of 125 km for Earth and Mars, and at 250 km for Venus, considered to be the start of the noticeable atmospheres, and thus the entry interface. The target of the aerocapture manoeuvre is a circular orbit with a radius of 500 km above the mean volumetric radius of the considered planet with the same inclination as the initial orbit.

III. Entry Corridor

A. Methodology

The range of applicability for the optimal aerocapture manoeuvre can be expressed in the form of an entry corridor. The entry corridor encompasses the initial conditions for which optimal aerocapture can be achieved without violating the imposed constraints, i.e., the mechanical load factor and aerodynamic heating.

For arbitrary initial conditions an optimal aerocapture is possible when the trajectory that minimises the loads does not violate the constraints, the trajectory that maximises the skip-out altitude does not undershoot the target altitude, and the trajectory that minimises the skip-out altitude does not overshoot the target.

Three considerations form the basis of studying aerocapture:[14]

1. Peak load factor and heat flux occur during the descending leg of the trajectory.
2. Lift-up minimises the peak load factor and heat flux and maximises skip-out altitude.
3. Lift-down maximises the peak load factor and heat flux and minimises skip-out altitude.

With this in mind, it can be shown that for arbitrary initial conditions, optimal aerocapture is only possible if the full lift-up trajectory both respects the constraints and touches or overshoots the target, and the full lift-down trajectory touches or undershoots the target. If any of these is not true, optimal aerocapture is not possible.

[a]TU Delft Astrodynamic Toolbox website available at http://tudat.tudelft.nl/

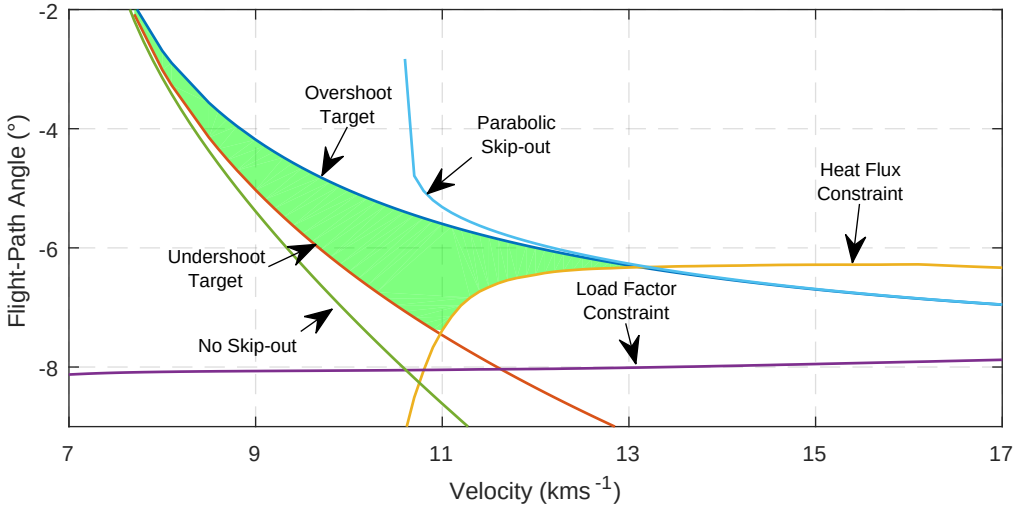

Figure 1. Altitude-targeting entry corridor for the Earth-CRM case, flown with nominal vehicle configuration.

By determining the initial conditions for which the full lift-up trajectory or full lift-down trajectory touches the target, or for which the loads experienced during the full lift-up trajectory matches the constraints, the boundaries for the entry corridor can be established. In addition to these four boundaries, two others are added simply to provide additional insight into the entry corridor. These two boundaries are the no-skip out boundary for the lift-up case, and the parabolic skip-out boundary for the lift-down case. As the names imply, these boundaries are those initial conditions for which the vehicle either no longer skips out (remains within the atmosphere), or is not successfully captured.

It should be noted that due to the inclusion of the lift-down trajectory boundaries, the set of initial conditions contained within the boundaries do not guarantee that an optimal trajectory is possible. However, being outside the boundaries does guarantee that an optimal trajectory is impossible without a ΔV manoeuvre either prior to entry, or post-exit.

To illustrate this, consider the point where a boundary flown full lift-down, such as "overshoot target", and a boundary flown full lift-up, such as "heat-flux constraint", intersect. At this point the trajectory has to be flown full lift-up to prevent violating the constraints, but to avoid guaranteed overshoot, the trajectory has to be flown lift-down. This contradiction gives rise to an impossible trajectory requirement.

To remedy this, a slight change can be made to the definition of the lift-down boundaries by using the fact that the peak loads occur on the descending leg. Instead of performing a full lift-down flight, one can perform lift-up flight until horizontal, and then switch to lift-down, such that the entire descending leg is flown lift-up. This will result in minimised loads, so that there is no longer a contradiction. This version of the entry corridor is hereinafter referred to as the "direct-entry entry corridor", to distinguish it from the altitude-targeting entry corridor. This corridor has applications for a direct-entry mission as well, as will be discussed later.

B. Altitude Targeting Entry Corridor

In Fig. 1 the entry corridor for the Earth-CRM case is shown. In this figure the green area indicates the upper bound for the entry corridor width. Just to reiterate, having initial conditions within this area does not guarantee an optimal trajectory, however, initial conditions outside this area guarantee that an optimal trajectory is impossible.

Entry corridors are also produced for the Mars-CRM and Venus-CRM cases. These can be seen in Fig. 2. In addition to the entry corridors, the bottom right graph shows the width of the individual entry corridors as a function of initial velocity. This facilitates comparing the size of the entry corridors. By showing all the graphs side by side, one can easily compare the position and size of each one of them. The corridors for Earth and Venus are comparable in terms of velocity and width, but for aerocapture on Venus one must enter on a shallower path due to the higher density at Venus, compared to Earth and Mars. The Mars corridor is significantly broader, and requires a significantly steeper entry to prevent overshooting the target or skipping out without being captured.

For entry with low velocity, the flight-path angle boundaries are driven by the full lift-up undershoot and the full lift-down overshoot boundaries. The imposed trajectory constraints become only driving when the velocity increases, which leads to larger peak load factor and heat flux. For the Earth-CRM

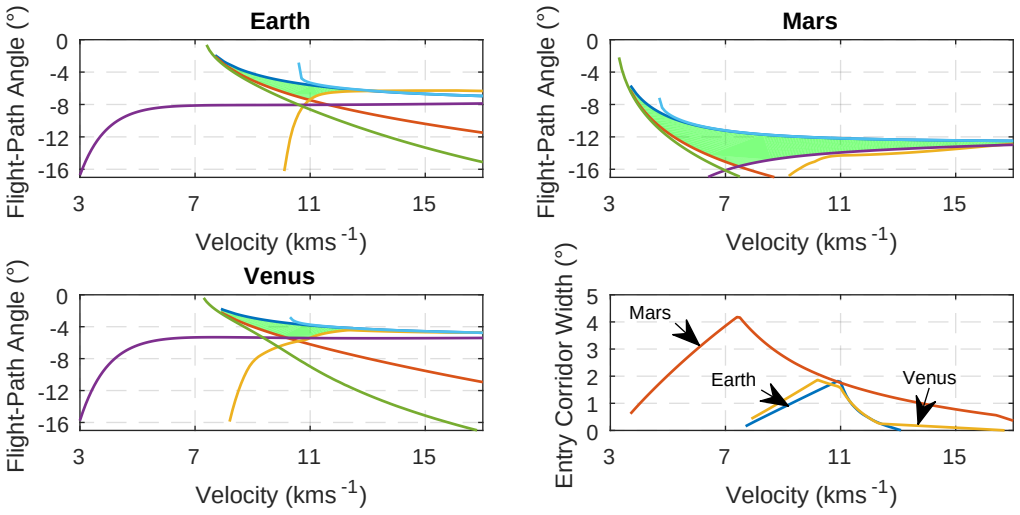

Figure 2. Comparison between the altitude-targeting entry corridors for all three planets, flown with nominal CRM configuration.

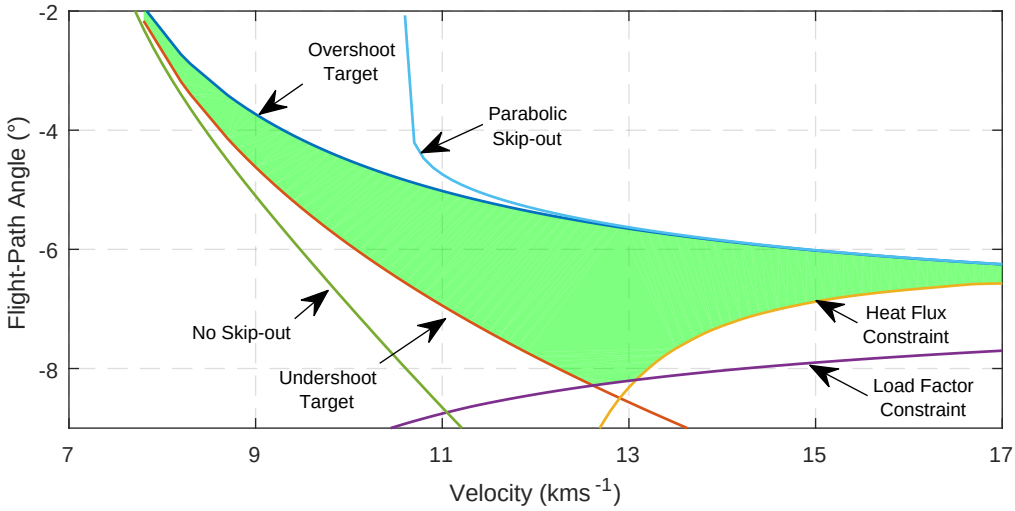

Figure 3. Nominal entry corridor for Earth-SRM case with nominal vehicle configuration.

case, the load factor is never a driving constraint, as the heat-flux constraint is more demanding with increasing velocity.

For Mars the opposite conclusion can be drawn. Here, the peak heat flux never becomes a driving constraint, but the peak load factor dictates the maximum steepness of the entry. Venus shows a combination of both. For low initial velocities, the undershoot boundary is driving, which gets surpassed by the load-factor boundary as the velocity increases, and gets surpassed by the heat load as the velocity continues to increase.

In Fig. 3 the entry corridor for the Earth-SRM case is shown. By comparing this figure to Fig. 1, it can immediately be observed that the entry corridor for the SRM is larger than the corridor for the CRM. This is due to the relaxed constraints regarding the load factor compared to the CRM, and the vehicle having a smaller nose radius. The smaller nose radius increases the convective heat flux and decreases the radiative heat flux. Since it was found that during aerocapture the radiative heat flux is generally larger than the convective heat flux, the smaller nose radius results in a lower total heat flux. This trait is not only observed when comparing the CRM and SRM cases for Earth, but also for Mars and Venus.

Similar to the CRM case, the entry corridors for the Mars and Venus SRM are compared with the one for Earth in Fig. 4. It can again be seen that the entry corridors for Earth and Venus have comparable velocity ranges and corridor widths, but a shallower entry is dictated for Venus, and that the Mars entry corridor is significantly larger, but requires a steeper entry. From the corridor width it can easily be

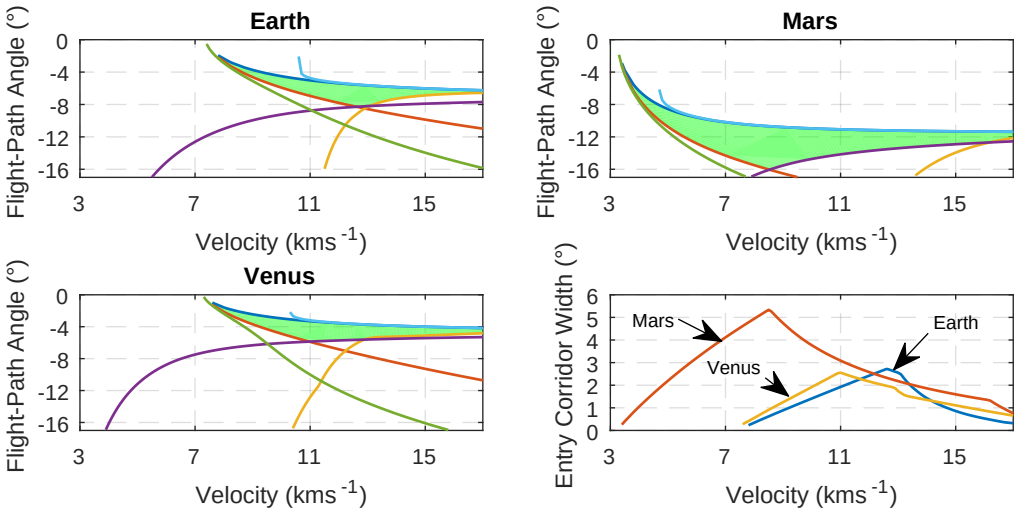

Figure 4. Comparison between the altitude-targeting entry corridors for all three planets, flown with nominal SRM configuration.

concluded that the entry corridors for the SRM are much larger than for the CRM.

Unlike the Mars-CRM case, for the Mars-SRM case, the peak heat flux becomes a driving constraint at the highest simulated velocities. This might be difficult to see in the top right graph in Fig. 4 depicting the Mars entry corridor, but can be seen from the discontinuity on the Mars entry corridor width in the bottom right graph.

The Venus-SRM case is similar to the Venus-CRM case in that first the undershoot boundary is dominant, followed by the load-factor boundary and finally the heat-flux boundary. The only difference is that in the SRM case the load-factor boundary is driving for a larger velocity range.

C. Direct-Entry Entry Corridor

As stated, the direct-entry entry corridor is defined sightly different from the altitude-targeting entry corridor. The direct-entry entry corridors for the Earth CRM and SRM cases are shown in Figs. 5 and 6, respectively. Three observations of these entry corridors can be made.

First, the undershoot target boundary is gone, as there is no longer a target to undershoot. Second, the no-skip-out boundary is not considered driving (and therefore dashed), because for direct-entry not skipping out of the atmosphere is not an issue. Third, the "Overshoot Target" boundary has been renamed to "Overshoot Max Altitude" to illustrate its applicability for a skipping entry flight with a maximum skip-out altitude. In this example, the maximum allowed skip-out altitude is put at the same altitude as the target orbit, i.e., 500 km.

By defining the upper-limit boundaries as described previously, the space encompassed by this entry corridor guarantees that direct-entry is possible without skipping out excessively high, and, more importantly, that optimal altitude-targeting aerocapture is guaranteed to be possible. A trajectory with initial conditions within these boundaries is guaranteed to be able to perform optimal aerocapture. However, in this case a region where aerocapture is potentially possible, although not guaranteed, is excluded. Therefore, the direct-entry entry corridor presented here can also be considered to be a conservative, guaranteed-aerocapture entry corridor. On the other hand, the altitude-targeting entry corridor shows the entire possible region, but without guarantees. The direct-entry entry corridors for the other two planets are shown in Figs. 7 and 8 for the CRM and SRM, respectively.

Initial conditions within these regions may lead to guaranteed aerocapture, as explained as follows. At the maximal skip-out and parabolic skip-out boundary, the vehicle has both a descending and ascending leg, otherwise the vehicle would not leave the atmosphere. The entire descending leg is flown lift-up, resulting in the minimum peak load factor and peak heat load. This means that there is no longer a contradiction at the intersection between the upper parabolic and overshoot boundaries, and the lower peak load-factor and heat-flux boundaries.

By combining the information from the altitude-targeting entry corridors presented in the previous section and the direct-entry entry corridors presented in this section, for any initial state it can be determined whether aerocapture is impossible (outside altitude-targeting corridor), potentially possible, to be determined by an optimisation scheme (inside altitude-targeting corridor, but not inside the direct-

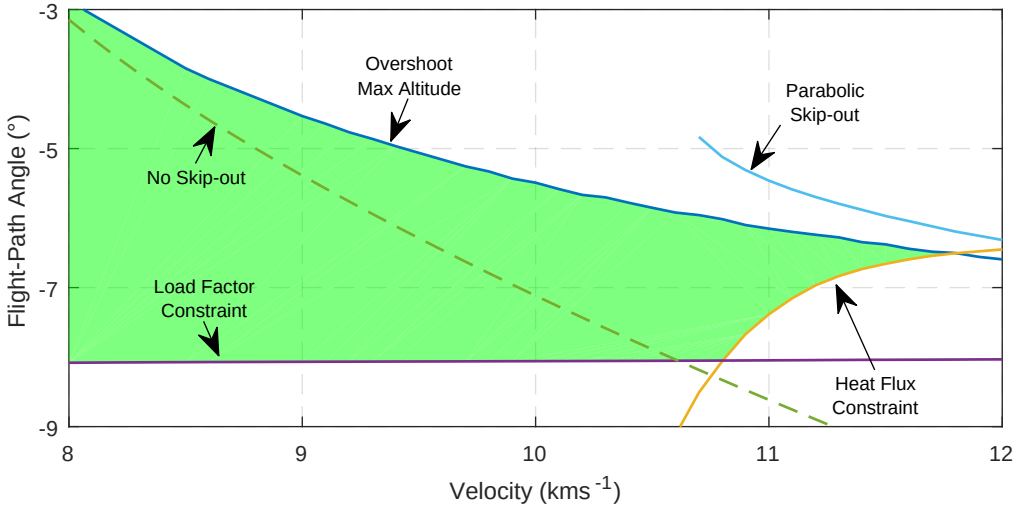

Figure 5. Range-targeting and guaranteed-safety altitude-targeting entry corridor for the Earth-CRM case, flown with nominal vehicle configuration.

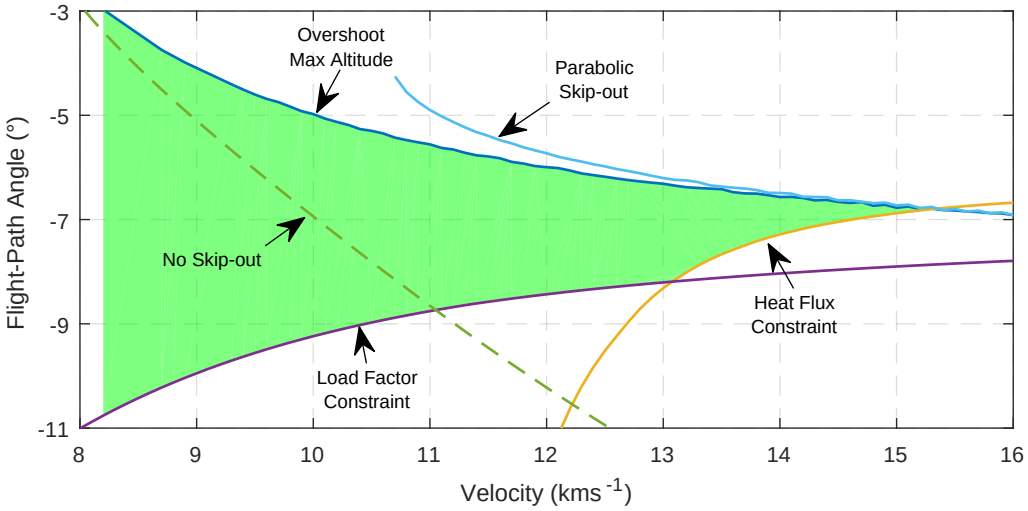

Figure 6. Range-targeting and guaranteed-safety altitude-targeting entry corridor for the Earth-SRM case, flown with nominal vehicle configuration.

entry entry corridor), or guaranteed possible (inside direct-entry entry corridor). This is visualised in Fig. 9, where the altitude-targeting and direct-entry entry corridors are overlapped, and the regions for guaranteed and potentially possible aerocapture are shaded green and yellow, respectively.

D. Entry-Corridor Variations

In this section the effect of varying the vehicle configuration on the entry corridor is investigated. The two aspects of the vehicle configuration that are altered are the aerodynamic model and the vehicle mass. As the variation in the vehicle configuration has the same effect for all six cases and for both altitude-targeting and direct entry, at least in a qualitative manner, only the altitude-targeting Earth-CRM case will be shown in detail. For the other cases, only the impact on the area bounded by the entry corridor will be shown. The area bounded by the entry corridor is obtained by integrating the area between the upper and lower bound. By comparing the rates of change of the areas, conclusions can be drawn regarding the sensitivity of the entry corridor to the vehicle configuration.

1. Aerodynamics

The first aspect of the vehicle model that is varied is the aerodynamic model. This model is altered in two different ways. The first way is to scale the lift coefficient up and down by 20%. As the vehicle

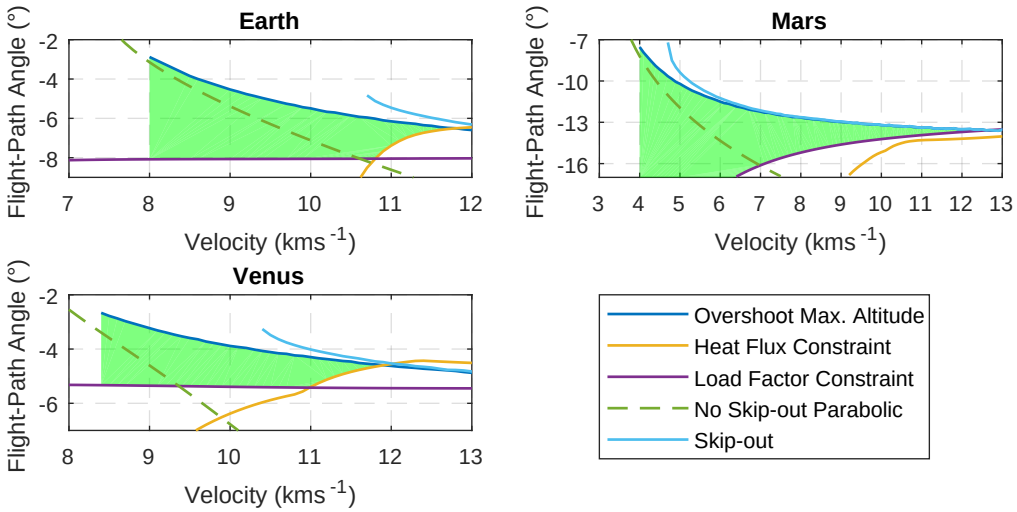

Figure 7. Range-targeting and guaranteed-safety altitude-targeting entry corridor for the CRM for all planets, flown with nominal vehicle configuration

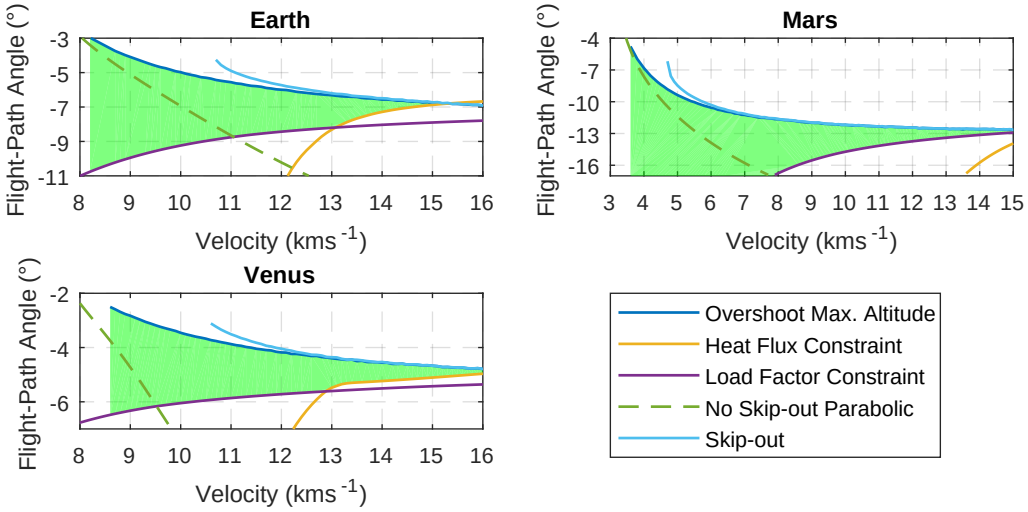

Figure 8. Range-targeting and guaranteed-safety altitude-targeting entry corridor for the SRM for all planets, flown with nominal vehicle configuration

model shown in Table 1 has a variable L/D, this method retains the variable L/D nature of this model. The effect of increasing and decreasing the lift coefficient on the entry corridor is illustrated in Fig. 10.

The result of increasing the lift-coefficient is an overall wider entry corridor. Because of the increased lift coefficient, during lift-up flight, the vehicle remains higher in the atmosphere, lowering the load factor and heat flux, compared to a nominal flight with the same entry angle, thus allowing for a steeper entry. As it flies higher in the atmosphere, the aerodynamic forces, mainly drag, are smaller compared to the nominal situation, and thus less velocity is lost. The vehicle can therefore enter steeper and still manage to skip out and reach its target. For lift-down flight, as the vehicle generates more lift "pulling" the vehicle down, a shallower entry can be performed that still results in capture. Naturally, the effect of lowering the lift-coefficient is the opposite.

The effect on this lift variation on the size of the entry corridor is shown in Fig. 12 for the CRM, and in Fig. 14 for the SRM. The value for the entry corridor area in these figures has been normalised with respect to the nominal area.

In addition to the effect scaling the lift-coefficient, the effect of varying the L/D ratio is also investigated. By keeping the drag-coefficient dependency on the velocity and making the corresponding lift-coefficient a multiplication of these values, a fixed L/D profile is obtained. The L/D of the vehicle is varied from $L/D = 0$, ballistic entry, to $L/D = 3$. In addition, the L/D ratios of 0.26 and 0.44 are also used. These values are chosen as they represent the minimum and maximum L/D ratio of the variable L/D profile. The effect on the entry corridor area for the CRM and SRM can be seen in Fig. 11 and

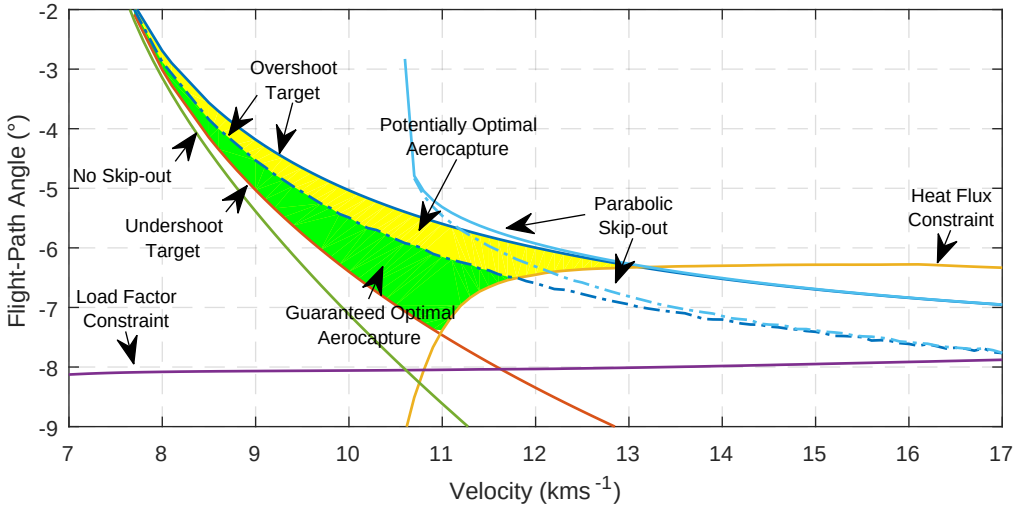

Figure 9. Combined entry corridor showing the region for optimal aerocapture, and the region for which aerocapture is potentially possible.

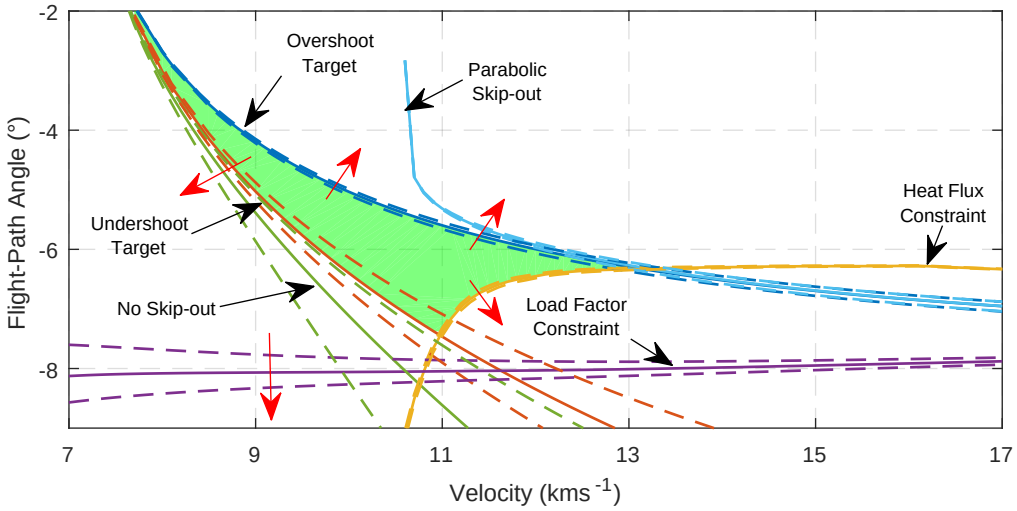

Figure 10. Altitude-targeting entry corridor for the Earth-CRM case, flown with lift variations of vehicle configuration. The red arrows indicate the direction of increasing lift.

Fig. 13, respectively

These figures show that, as L/D increases, the entry corridor seems to become less sensitive to the increase in L/D. This is especially pronounced for the Mars cases. However, for Mars, this is a misleading observation, as the sudden decrease in sensitivity is not due to an actual decrease in sensitivity, but due to the range of initial conditions for which the entry corridor is produced. This range imposes artificial boundaries on the entry corridor size that limit the maximal entry corridor area.

As the entry corridor for Mars is much closer to two of these boundaries (steepest flight-path angle and slowest velocity), the entry corridor cannot be increased as much as for Venus and Earth. For the latter planets these limits are not reached even at $L/D = 3$, and it can thus be concluded that the sensitivity to L/D decreases as for larger L/D. So, increasing the L/D of a low L/D vehicle has an overall positive effect on the size of the entry corridor, but the effectiveness of increasing the L/D decreases for vehicles with high L/D ratios.

2. Mass

The second investigation is into the effect of the mass on the vehicle on the entry corridor. Similar to the lift variation, the mass is varied by ±15%. The effect of the mass variation on the entry corridor for the Earth-CRM case is shown in Fig. 15.

The vehicle mass affects the entry corridor in a different way than the lift did. The mass variation

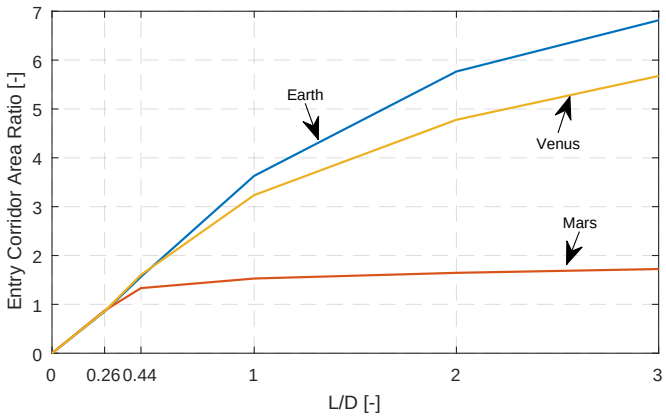

Figure 11. Effect on the altitude-targeting entry corridor area due to variation of L/D for the CRM.

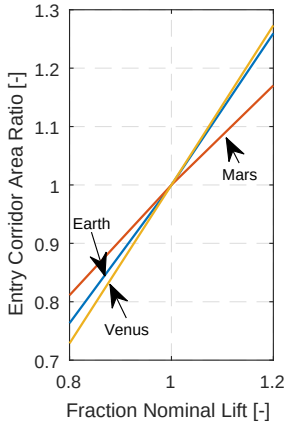

Figure 12. Effect on the altitude-targeting entry corridor area due to variations in the lift for the CRM.

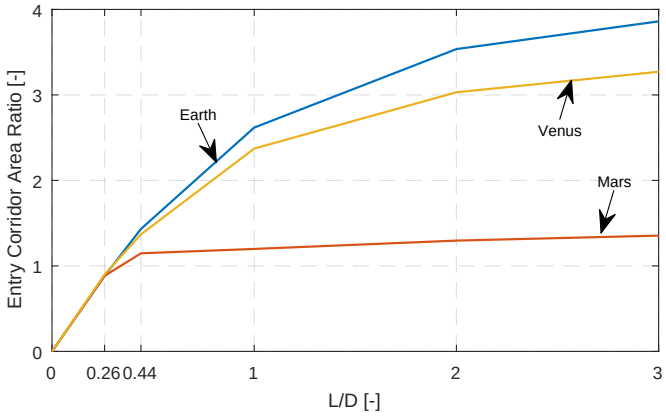

Figure 13. Effect on the altitude-targeting entry corridor area due to variation of L/D for the SRM.

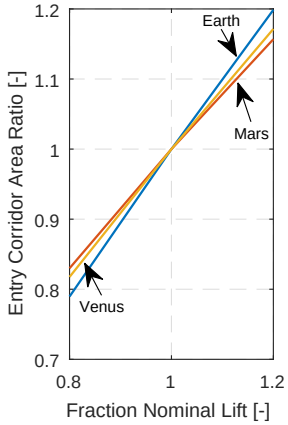

Figure 14. Effect on the altitude-targeting entry corridor area due to variations in the lift for the SRM.

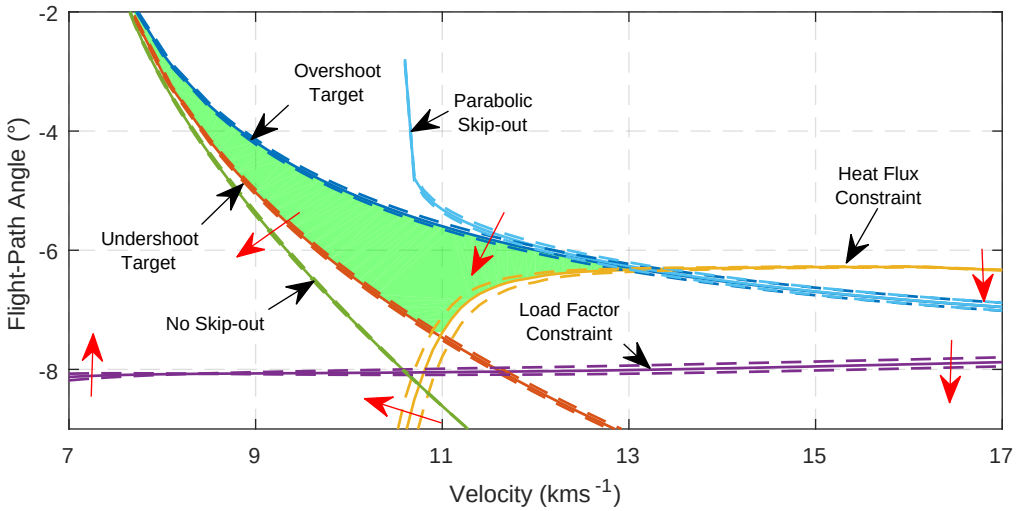

Figure 15. Altitude-targeting entry corridor for the Earth-CRM case, flown with mass variations of vehicle configuration. The red arrows indicate the direction of increasing mass.

causes more of a shift of the entry corridor instead of a widening. The no-skip, undershoot, overshoot, and parabolic skip boundaries all shift in the same direction, and either a steeper entry is possible (in

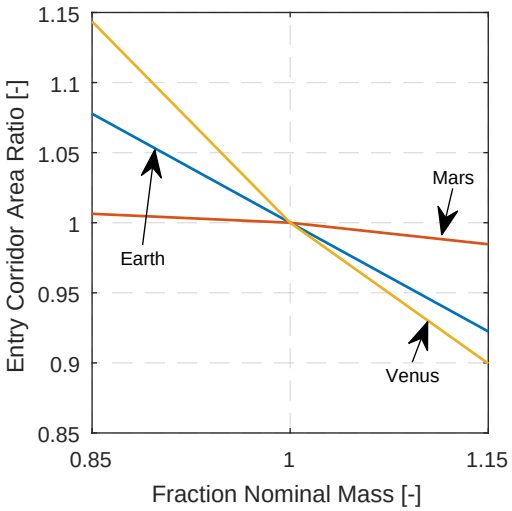

Figure 16. Effect on the altitude-targeting entry corridor area due to variations in the mass of the CRM.

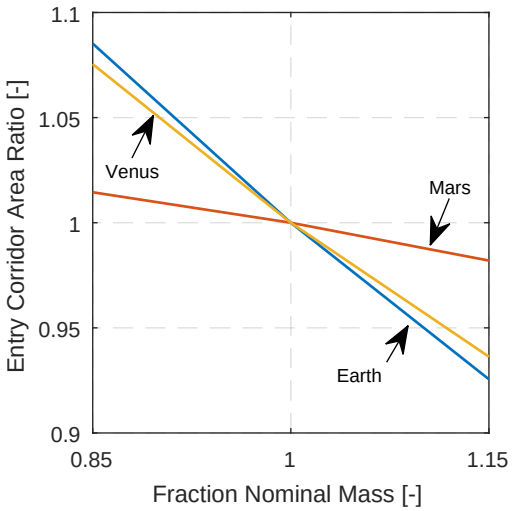

Figure 17. Effect on the altitude-targeting entry corridor area due to variations in the mass of the SRM.

case of the former two) or required (in case of the latter two) when the mass increases.

The change in peak heat-flux has the largest impact on the entry-corridor area. For the velocities relevant to the entry corridor, the peak heat flux increases compared to the nominal configuration. Due to the lower aerodynamic accelerations the vehicle will reach a lower point in the atmosphere with a higher velocity, as compared to the nominal situation.

With increasing velocity, the effect of mass variations on the heat-flux boundary disappears. At these high velocities, and with the flight-path angle indicated by the heat-flux boundary, the vehicle does not penetrate deep enough due to the high rate of change of the flight-path angle, resulting in negligible aerodynamic acceleration.

The effect of this mass variation on the size of the entry corridor is shown in Fig. 16 for the CRM, and in Fig. 17 for the SRM. Again, the value for the entry-corridor area in these figures has been normalised with respect to the nominal one. Comparing the entry-corridor ratios in these figures to those in Figs. 12 and 14, it can be determined that the entry corridor is less sensitive to changes in mass than to changes in the aerodynamics. Additionally, the sensitivities for the individual planets seem to differ significantly more than they did for lift. It can therefore be concluded that to increase the entry corridor area, it is more efficient to increase the lift while keeping the mass the same. Even if the mass of the vehicle had to increase, the total effect on the entry corridor might still be positive, although the increase in mass is counter-productive to the purpose of the aeromanoeuvre.

IV. Optimal Aerocapture Trajectories

Thus far, the entry corridors that encompass the initial conditions for which optimal aerocapture is possible, either potentially or guaranteed, have been introduced, and the effect of varying the vehicle configurations on them has been analysed. In this section a method for determining the optimal aerocapture trajectory for arbitrary initial conditions is developed. Following this, some results of the optimisation process are presented.

A. Optimisation Method

Similar to the methodology for determining the entry corridor, first three observations are stated, namely:

1. In a simplified situation, the bang-bang trajectory minimises the ΔV_{total} required for aerocapture.[15]
2. For an arbitrary initial condition and a lift-up, lift-down, bang-bang trajectory, ΔV_2 behaves monotonically with varying switch time
3. For an arbitrary initial condition and a lift-up, lift-down, bang-bang trajectory, if the root of ΔV_2 exists, it coincides with the minimal ΔV_{total}

Since a bang-bang trajectory minimises ΔV, and a lift-up trajectory minimises the loads experienced during the atmospheric flight, a lift-up, lift-down bang-bang trajectory will result in both minimised

loads and minimised ΔV for aerocapture. This results in an optimisation problem where the only design variable is the switch time, t_s. The switch time is the time when the commanded bank angle switches from 0 deg (lift-up) to 180 deg (lift-down).

As the minimum ΔV_{total} coincides with the root of ΔV_2, and ΔV_2 behaves monotonically – and therefore has at most one root – this problem reduces to a relatively simple root-finding problem rather than being an optimisation problem.

To ascertain that ΔV_2 has a root, two nodes must be found where the corresponding ΔV_2 values have opposite signs. When these are found, the root is located somewhere on the interval bounded by the two nodes. By simulating the trajectory twice for each of the two extreme values of the switch time, the existence of the required root can be determined. The extreme values of the switch time are $t_s = 0$ and $t_s = \infty$. These two switch times correspond to full lift-down and full lift-up trajectories, respectively. This step is equivalent to determining if the initial conditions are within the entry corridor by determining if the trajectory overshoots the target (negative ΔV_2) for full lift-up flight, and undershoots the target (positive ΔV_2) for full lift-down flight.

If the two nodes have opposite signs, and the full lift-up trajectory did not violate the constraints, the initial conditions fall within the entry corridor, and it can thus be attempted to develop the optimal aerocapture trajectory by finding the value of t_s for which $\Delta V_2 = 0$.

Since no derivatives of ΔV_2 with respect to t_s are known, the root-finding schemes available are limited. For this research the simple bisection method was chosen for its simplicity. By setting the maximal allowed absolute value of $\Delta V_2 = 0.01$ m/s, and a minimal interval width of 10^{-10} s, an estimate for the root of ΔV_2 can be obtained.

To significantly decrease the interval for the root finding, $t_s = \infty$ can be replaced by the time at which the full lift-up trajectory left the noticeable atmosphere, t_f, as switching after this time has no effect on the trajectory. Additionally, $t_s = 0$ can be replace by t_p, the time the vehicle reaches the point of deepest penetration, as it was found that usually the optimal switch time occurred on the ascending leg. Doing this also guarantees that the peak loads are minimised, because the entire descending leg is flown lift-up.

In the rare case where the root is not within this interval, but does exist, $t_s \in [0, t_p]$ should be used. However, it could be that the found t_s that corresponds to the root of ΔV_2 results in a trajectory that violates the constraints, as the loads are no longer minimised. In this case one can either accept the violated constraints, attempt to find a switch time for which the constraints are respected and accept a sub-optimal aerocapture, or change the initial conditions of the aerocapture.

B. Optimisation Results

The above methodology is used to analyse if aerocapture is possible for a wide range of initial conditions for every planet and vehicle considered in this research. If it is determined that aerocapture is possible, the trajectory is optimised and the required ΔV_2 to obtain the target apoapsis is determined. In case optimal aerocapture is not possible, a post-exit two-burn ΔV manoeuvre will be used to obtain a measure for the required ΔV. In the optimal situation $\Delta V_2 = 0$, for an overshoot $\Delta V_2 < 0$, and for an undershoot $\Delta V_2 > 0$.

In Figs. 18, 19, and 20, the ΔV_2 is shown for the flight with the CRM vehicle. Each of these figures contains two graphs. The left graph shows a three-dimensional surface plot of the ΔV_2 required to correct the orbit after aerocapture has been performed. The right graph shows the top-down projection of this surface. Additionally, the altitude-targeting entry-corridor boundaries are present in the top-down view. This facilitates comparing the initial conditions where optimal aerocapture is potentially possible according to the entry corridor to those where an optimal aerocapture is found to be possible.

In these figures the red-shaded area indicates an undershoot, corresponding to a positive ΔV_2, the yellow/orange-shaded area correspond to an optimal aerocapture, with $\Delta V_2 \approx 0$, and lastly the blue shaded-areas indicate an overshoot, corresponding to a negative ΔV_2. As only post-exit ΔV manoeuvres are considered, no values are present for initial conditions that either violate the constraints, fail to skip out, or skip out hyperbolically.

By comparing the entry-corridor boundaries and the transitions from undershoot (positive ΔV_2) to optimal ($\Delta V_2 \approx 0$) to overshoot (negative ΔV_2), it can be concluded that the altitude-targeting boundaries approximate the limit initial conditions very well, even though they do not guarantee that entry is possible within their bounds. Additionally, it can be concluded that the methodology described above does indeed result in the development of optimal trajectories, granted that the initial conditions allow for such a trajectory.

From these figures it can also be concluded that the post-exit apoapsis is highly sensitive to changes in both initial velocity and flight-path angle, visualised by the steep slope. The ΔV_2 required for a post-

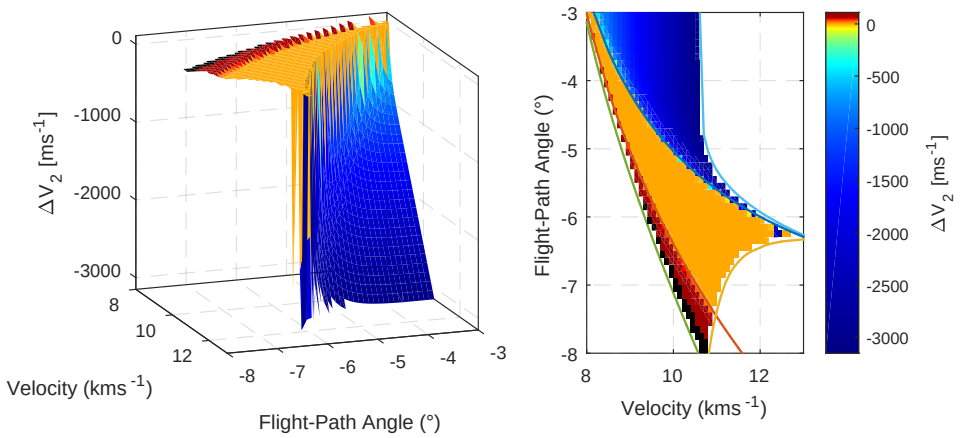

Figure 18. ΔV_2 **required to reach the target apoapsis for the Earth-CRM altitude targeting case for a wide variety of initial conditions.**

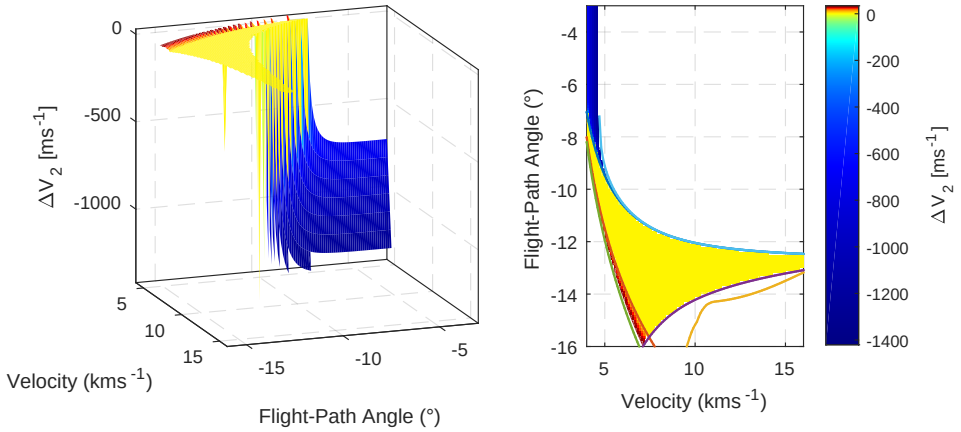

Figure 19. ΔV_2 **required to reach the target apoapsis for the Mars-CRM altitude targeting case for a wide variety of initial conditions.**

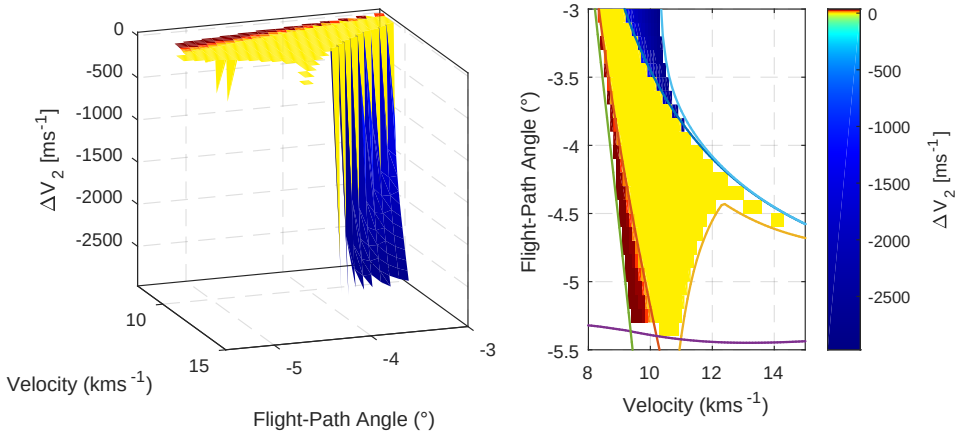

Figure 20. ΔV_2 **required to reach the target apoapsis for the Venus-CRM altitude targeting case for a wide variety of initial conditions.**

exit orbit correction increases significantly faster for the overshoot cases, requiring significantly more ΔV compared to the undershoot corrections. However, this can be alleviated by employing the concept of aerobraking, which is expected to significantly reduce the ΔV required for correcting these orbits.

V. Conclusions and Recommendations

It has been demonstrated that the relatively simple lift-up-lift-down bang-bang trajectory is the most optimal type of trajectory for altitude-targeting aerocapture. It was furthermore shown that the optimal switch-time at which this manoeuvre should be executed can be determined by using a straight-forward bisection method of root finding, using the post-exit ΔV_2 as the parameter to be made zero.

For all vehicle and planet combinations considered, two types of entry corridors have been developed. The first of these corridors marks two limits of initial conditions for which aerocapture could potentially be performed. Due to the nature of this first type of corridor, being inside the boundaries does not guarantee that aerocapture is possible, but being outside of it does make it impossible. A second, more conservative version of the entry corridor was also developed. This entry corridor has the opposite effect compared to the first. Being inside the boundaries specified by this corridor guarantees that optimal aerocapture is possible, however, being outside of the boundaries does not mean aerocapture is impossible. It was also found that the first, non-guaranteeing entry corridor predicted the range of initial conditions, for which aerocapture is possible, remarkably well. Only the limit cases, such as the intersection between two opposite borders, resulted in non-optimal aerocapture.

In case the vehicle fails to skip out of the atmosphere, or violates a constraint in the full lift-up condition a pre-entry ΔV manoeuvre must be executed to salvage the trajectory. A single ΔV may alter the initial conditions, such that an optimal trajectory is obtained with $\Delta V_2 = 0$. Alternatively, a two-burn manoeuvre may be required to obtain the desired circular orbit. Which of these two methods is optimal, together with determining the magnitude and direction of the ΔV manoeuvres, is left as future research.

This work only focussed on the optimisation of altitude-targeting aerocapture. An obvious recommendation for future work is the optimisation of direct-entry aerocapture or skipping aerocapture. In this research the flight envelopes for this type of entries have been developed, but an optimal trajectory that would fall within this envelope has not.

The last recommendation made is to study the possibility of combining the aerocapture and aerobraking manoeuvres, as this combination is expected to lead to a significant increase in the entry corridor width and decrease in the required ΔV for initial conditions that overshoot their target.

References

[1]Cruz, M.I., "The Aerocapture Vehicle Mission Design Concept". In *Proceedings of the Conference on Advanced Technology for Future Space Systems*, May 1979. DOI:10.2514/6.1979-893.

[2]Graves, C.A. and Harpold, J.C., "Re-Entry Targeting Philosophy and Flight Results from Apollo 10 and 11". In *Proceedings of the 8th Aerospace Sciences Meeting*, January 1970. DOI:10.2514/6.1970-28.

[3]O'Neil, W.J. and Cazaux, C., "The Mars Sample Return Project". *Acta Astronautica*, 47(2-9):453–465, 2000. DOI:10.1016/S0094-5765(00)00085-0.

[4]Robinson, J.S., Wurster, K.E., and Mills, J.C., "Entry Trajectory and Aeroheating Environment Definition for Capsule-Shaped Vehicles". *Journal of Spacecraft and Rockets*, 46(1):74–86, January-February 2009. DOI: 10.2514/1.30998.

[5]Picone, J. M., Hedin, A. E., Drob, D. P. and Aikin, A. C., "NRLMSISE-00 empirical model of the atmosphere: Statistical comparisons and scientific issues". *Journal of Geophysical Research: Space Physics*, December 2002. DOI: 10.1029/2002JA009430

[6]Millour, E., Forget, F., Spiga, A., Vals, M., Zakharov, V., Montabone, L., Lefevre, F., Montmessin, F., Chaufray, J.Y., López-Valverde, M.A., González-Galindo, F., Lewis, S.R., Read, P.L., Desjean, C.C., and Cipriani, F., "The Mars Climate Database (Version 5.3)". Scientific Workshop: "From Mars Express to ExoMars", February 2018.

[7]Justh, H.L., Justus, C.G., and Keller, V.W., "Global Reference Atmospheric Models, Including Thermospheres, for Mars, Venus and Earth," in *Proceedings of the AIAA/AAS Astrodynamics Specialist Conference & Exhibit*, August 2006. DOI: 10.2514/6.2006-6394

[8]Sutton, K. and Graves, Jr., R.A., "A General Stagnation-Point Convective-Heating Equation For Arbitrary Gas Mixtures". Technical report R-376, National Aeronautics and Space Administration, November 1971.

[9]Anderson, Jr, J.D., *Hypersonic and High-Temperature Gas Dynamics - Second Edition*. AIAA Education Series. 2006.

[10]Carandente, V., Savino, R., Iacovazzo, M., and Boffa, C., "Aerothermal Analysis of a Sample-Return Reentry Capsule". *FDMP: Fluid Dunamics& Materials Processing*, 9(4):461–484, 2013. DOI:10.3970/fdmp.2013.009.461

[11]Detra, R.W. and Hidalgo, H., "Generalized Heat Transfer Formulas and Graphs for Nose Cone Re-Entry Into the Atmosphere". *ARS Journal*, 31(3):318–321, January 1961. DOI:10.2514/8.5471.

[12]Tauber, M.E. and Sutton, K., "Stagnation-Point Radiative Heating Relations for Earth and Mars Entries". *Journal of Spacecraft and Rockets*, 28(1):40–42, January-February 1991. DOI:10.2514/3.26206.

[13]Craig, S. and Lyne, J.E., "A Paramteric Study of Aerocapture for Missions to Venus". In *Proceedings of the AIAA Atmospheric FlightMechanics Conference*, August 2002. DOI:10.2514/6.2002-4500.

[14]Zucchelli, E.M. and Mooij, E., "Minimum Radiative Heat-load Aerocapture Guidance with Attitude-Kinematics Constraints". *2018 AIAA Guidance, Navigation, and Control Conference*, January 2018, DOI:10.2514/6.2018-1319

[15]Lu, P., Cerimele, C.J., Tigges, M.A., and Matz, D.A., "Optimal Aerocapture Guidance". *Journal of Guidance, Control, and Dynamics*, 38(4):553–565, April 2015. DOI:10.2514/1.G000713.